Effect of High Pressure on the Second Harmonic Generation Efficiencies of Three Monoclinic Organic Compounds

Y. Li, G. Yang, Z. A. Dreger, J. O. White, and H. G. Drickamer*

School of Chemical Sciences, Department of Physics and The Frederick Seitz Materials Research Laboratory, University of Illinois, 600 S. Mathews Ave., Urbana, Illinois 61801-3792

Received: February 6, 1998; In Final Form: April 28, 1998

The effect of pressure to ∼90 kbar has been measured on the second harmonic generation (SHG) efficiency for the monoclinic crystals 4-aminobenzophenone (ABP), 4-Br-4′-methoxychalcone (BMC), and 2-methyl-4-nitroaniline (MNA). In ABP and BMC the SHG efficiency increases by 2−3 orders of magnitude with some dependence on orientation. The results can be explained qualitatively in terms of a decrease in Δk, the mismatch between the coupled fields, i.e., by pressure tuning of Δk. Powdered samples give much smaller increases in SHG efficiency but a clearer indication of first-order phase transitions, probably between point groups of the monoclinic structure. MNA crystal exhibits a very sharp increase in SHG efficiency by a factor ∼20 at pressures below 10 kbar. At pressures above ∼30 kbar self-absorption by the sample becomes dominant.

Introduction

Second harmonic generation (SHG) in organic crystals has been a subject of extensive investigation (see, e.g., refs 1−6 and references therein). Although the applications have been limited because of stability, fragility, and related problems, they are of both theoretical and potential technological interest.

Over the past four or five decades high pressure has proved to be a powerful tool for investigating and characterizing a wide variety of molecular and electronic phenomena. In a recent short paper[7] we presented preliminary and exploratory data on pressure effects for SHG in five organic crystals. In this paper we present considerably more refined results for three monoclinic crystals and some data on the corresponding powders. The compounds are 4-aminobenzophenone (ABP), 4-Br-4′-methoxychalcone (BMC), and 2-methyl-4-nitroaniline (MNA). Their structures are shown in Figure 1.

In addition, we present a brief discussion of how the rather large pressure effects in ABP and BMC in particular can be qualitatively explained in terms of the theory of SHG.

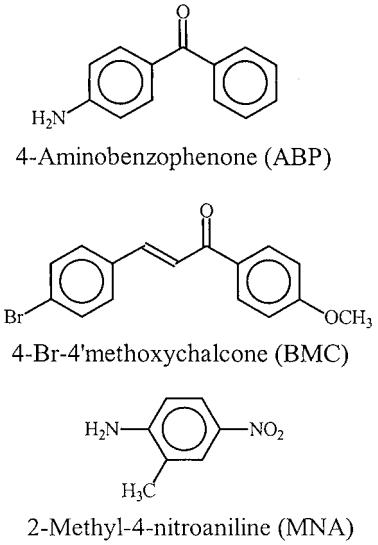

Figure 1. Structure of molecules studied.

Experiment

NLO grade 2-methyl-4-nitroaniline (MNA) was obtained from Chromophore Inc. and used without further purification. 4-Aminobenzophenone (ABP) was purchased from Aldrich and was purified by multiple recrystallizations from ethanol solution. 4-Bromo-4′-methoxychalcone (BMC) was synthesized in our laboratory according to a general method[8] and purified by multiple recrystallizations from ethanol. It is characterized by elementary analysis, and the expected result was obtained (C, 60.87%; H, 4.21%; Br, 25.52%; theoretical C, 60.59%; H, 4.13%; Br, 25.19%).

High pressure is generated in a Merrill-Bassett diamond anvil cell (DAC), utilizing low fluorescent and UV transmitting diamonds. The hole diameter of the gasket is approximately 0.3 mm. The sample and a tiny ruby chip are placed in the hole, and the pressure is determined by the fluorescence shift of the ruby chip.[9] A piece of aluminum foil is introduced between the sample (powder or a piece of single crystal) and the ruby chip to avoid damage to the sample during pressure measurement. Light mineral oil or glycerol is used as pressure medium, according to the solubility of the compounds.

The application of the DAC for high-pressure absorption experiments and the experimental setup have been described before.[10,11] The arrangement for the SHG measurement is shown schematically in Figure 2. A mode-locked Nd:YLF (neodymium-doped yttrium lithium fluoride) laser with a 76 MHz train of ∼50 ps pulses at 1053 nm is used as fundamental frequency source. The average power used in this work is 0.2−1.0 W, according to the SHG signal intensity of the sample at 1 atm, adjusted with an attenuator and detected by a powermeter (photodetector). A group of long-wavelength pass filters (F1) is inserted before the sample to cut off any light from the laser at 526.5 nm, and a group of long-wavelength cutoff filters (F2) is placed in front of the entrance of the photomultiplier tube (PMT) to block out the scattered fundamental frequency light. A waveplate (WP) with a vernier to measure the angle of

* To whom correspondence should be sent.

S1089-5647(98)01038-4 CCC: $15.00
Published on Web 07/10/1998

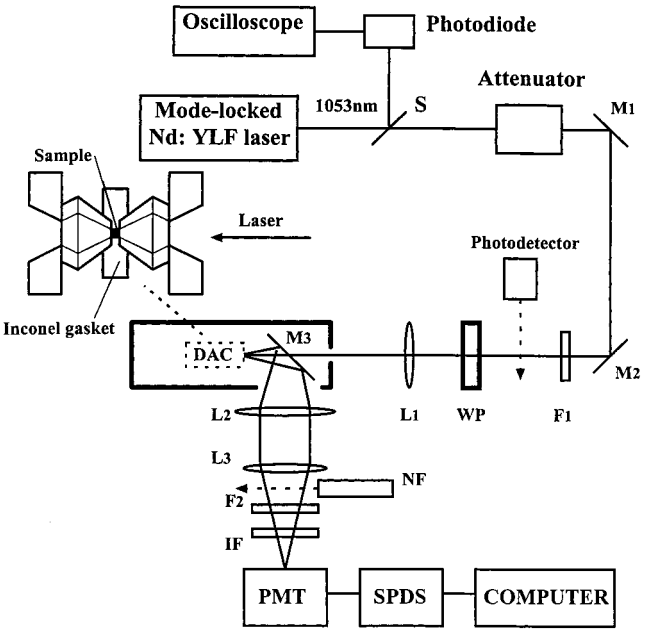

Figure 2. Diagram of apparatus for measuring SHG intensity as a function of pressure and angle of polarization of the laser beam: DAC, diamond anvil cell; M_1, M_2, M_3 (with a hole), mirrors; L_1, L_2, L_3, lenses; S, beam splitter; F_1, long-wavelength pass filter group; F_2, long-wavelength cutoff filter group; WP, waveplate; NF, calibrated neutral filter(s); IF, interference filter for 526.5 nm; PMT, photomultiplier; SPDS, single-photon detection system.

polarization of the laser beam is introduced in front of the sample to change the polarization of the laser light. Instead of a spectrometer, an interference filter (IF) for 526.5 nm was used in front of the PMT to avoid the possible effect of the grating on the polarized signal. The SHG signal (526.5 nm) generated by the 1053 nm laser is measured by the PMT coupled to a single-photon detection system (SPDS) and computer. The intensity at the photomultiplier tube is controlled by calibrated neutral density filters.

The powder used in this work had a particle size of less than 10 μm in any direction. The ABP and MNA single crystals were needles with a length of $\sim$80 μm and width and thickness $\sim$30 μm. The BMC platelets were $\sim 80 \times 80 \times 20\ \mu m^3$. To control the orientation, the needlelike or platelike crystal samples were loaded in the hole as identically as possible with a film of silicone grease to fix the position. After the high-pressure measurement the crystals maintained their original shape, but some inner cracks could be observed under a microscope.

Results

The results for ABP and BMC involve three types of measurements: (1) the SHG intensity as a function of angle of polarization of the laser beam at several pressures, (2) the change of intensity with pressure at one or more angles of polarization, and (3) data on the optical absorption as a function of pressure. The emphasis is on single-crystal behavior, but relevant information on powder samples is also included. The results for MNA are less extensive for reasons that will be clear in the presentation. As mentioned above, with the refined techniques used here, the crystals retained their external integrity and details of shape exactly.

For the crystals the relative SHG efficiency at atmospheric pressure (averaged over two sets of crystals and corrected for crystal size) was MNA/ABP/BMC = 39/25/1. Although, as indicated, an attempt was made to correct for crystal size, the

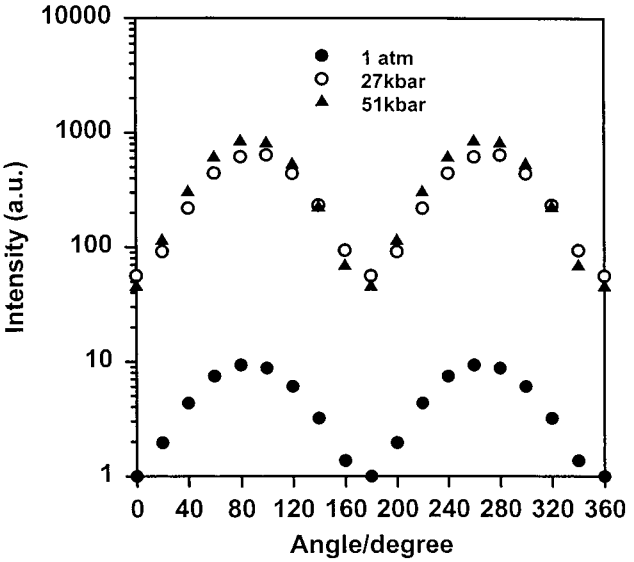

Figure 3. Typical SHG intensity as a function of polarization angle of the laser beam for ABP crystal at several pressures.

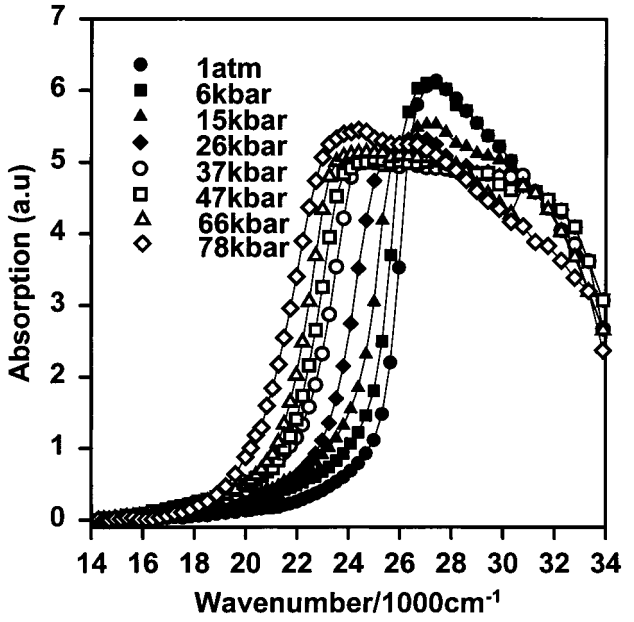

Figure 4. Optical absorption spectra vs pressure for ABP powder.

results are subject to error, especially for BMC, because of its different shape. For the powder the ratio MNA/ABP/BMC = 15.3/3.6/1. As discussed below, MNA undergoes a phase transition with a large increase in intensity. This transition initiates at a very low pressure, and it is probable that the process of grinding the powder converts MNA at least partially to the high pressure, high-intensity phase.

ABP. The results for ABP are presented in Figures3−6. As mentioned in the previous section, the crystals were needlelike and could be oriented with the long axis (the crystallographic *y* axis) in a fixed position in the cell. However, it was not possible to control the orientation in the plane perpendicular to the *y* axis. Most of the loads fell into one of two groups classified according to the change in intensity with pressure.

Figure 3 presents typical data for the change of intensity with angle of polarization of the laser beam (abbreviated as "angle" in the further discussion). There are two clear maxima $\sim$180° apart, with a minimum in between. The locations of the maxima and minimum are independent of pressure and of the crystal orientation in the plane perpendicular to the *y* axis. As can be

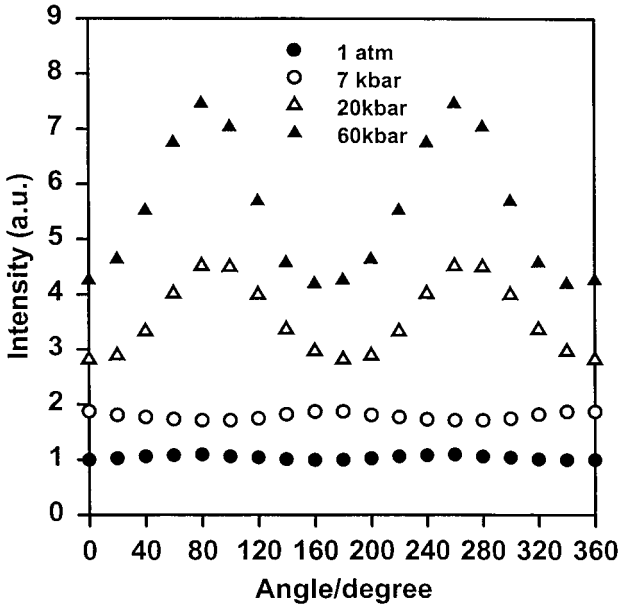

Figure 5. Typical SHG intensity as a function of polarization angle for ABP powder at several pressures.

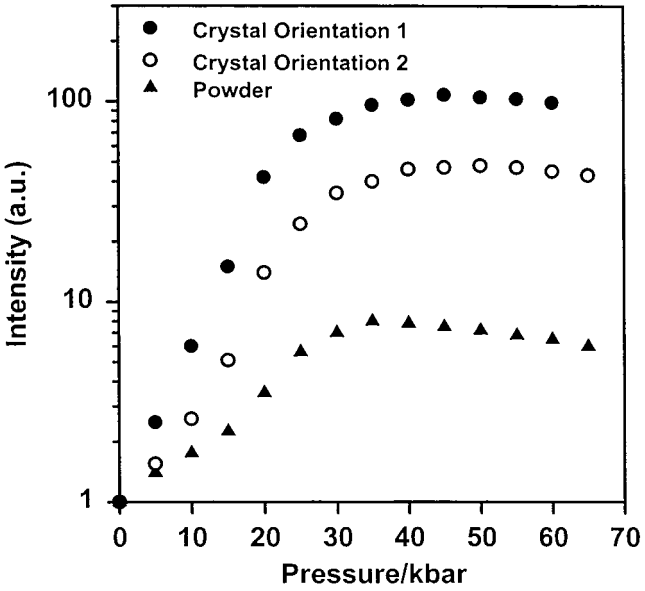

Figure 6. SHG intensity vs pressure (normalized to 1 atm value) for ABP (two crystal orientations) and the powder average value for several loads in each case.

estimated from Figure 3, the ratio of maximum to minimum intensity increases from about 10 to 20 from atmospheric pressure to 80 kbar.

Figure 4 presents optical absorption data on the powder. The peak shifts to lower energy with pressure. It should be noted that there is a clearly discontinuous red step shift near 25−35 kbar. Such shifts are almost always associated with phase transitions. A second indication of a transition can be seen in the powder data of intensity vs angle presented in Figure 5. Below 20 kbar the intensity is independent of angle as one would expect for powder. At higher pressure there is a modest but definite angular dependence (5−10% of that observed for the crystal). Evidently, the coherence length for ABP in the high-pressure phase is less than the powder dimensions so that one is measuring the behavior of an assembly of crystallites or probably focusing on a few of them.

Figure 6 presents the change in intensity of the SHG with pressure for the two orientations of the crystal and for the

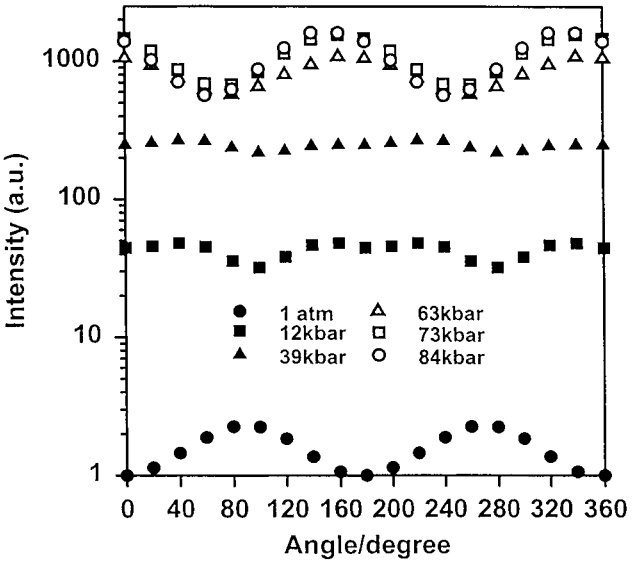

Figure 7. Typical SHG intensity as a function of polarization angle of the laser beam for BMC crystal for several pressures.

powder, averaged over 3−4 loads in each case. For orientation 1 the increase is by a factor of 100 ± 5; for orientation 2 the increase is by a factor of 50 ± 3. For the powder, the maximum increase is a factor of 8 ± 1. For the crystals in particular the change of intensity is measured at the angle giving maximum intensity at 1 atm.

It should be mentioned that all results for ABP were reversible upon release of pressure.

BMC. BMC, also a monoclinic crystal, demonstrates pressure behavior that is in some ways similar to ABP and in some ways quite different. The crystals are platelets of irregular shape. They were placed in the cell with the plate surface parallel to the diamond face. The crystallographic *z* axis is perpendicular to this face. The optical *z* axis is at a small angle to the crystallographic axis.[12] While the crystals were all inserted in the cell with the same apparent orientation, variations in the thickness (20 ± 5 μm) and possible surface smoothness on such thin crystals resulted in two somewhat different effects on the intensity change with pressure. We label them type 1 and type 2.

Figure 7shows typical data for the intensity as a function of angle at a series of pressures. Initially there are two maxima 180° apart as for ABP. Above about 60 kbar the maxima have moved 90° from their original position. In the region between ∼30 and 60 kbar there appears to be a mixture of the two angular dependencies so that the ratio of maximum to minimum intensity is small.

Because of the change of angle associated with the maxima and minima with pressure, it was felt desirable to consider the intensity increase with pressure for each type under two conditions. In Figure 8we show the increase at the angle that exhibited the maximum increase. The data for type 1 are the average of five loads and for type 2 the average of three loads. For type 1 the initial drop by a factor of 0.5 ± 0.1 is quite reproducible. The value at 90 kbar is 300 ± 30 times the initial value. For type 2 there is a steep initial rise, and the efficiency at 90 kbar is 1500 ± 150 times the 1 atm value.

In Figure 9we present the change of intensity with pressure starting from the maximum value at 1 atm. Qualitatively the features are the same as in Figure 8, but at 90 kbar the intensity increase for type 1 is by a factor of 55 ± 5, while for type 2 it is 300 ± 30.

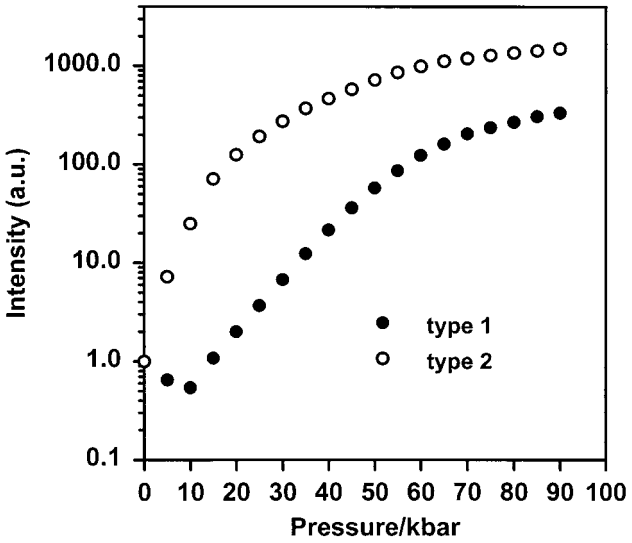

Figure 8. SHG intensity vs pressure (normalized to 1 atm value) for BMC at the angle giving maximum intensity increase—averaged over several loads for two crystal types.

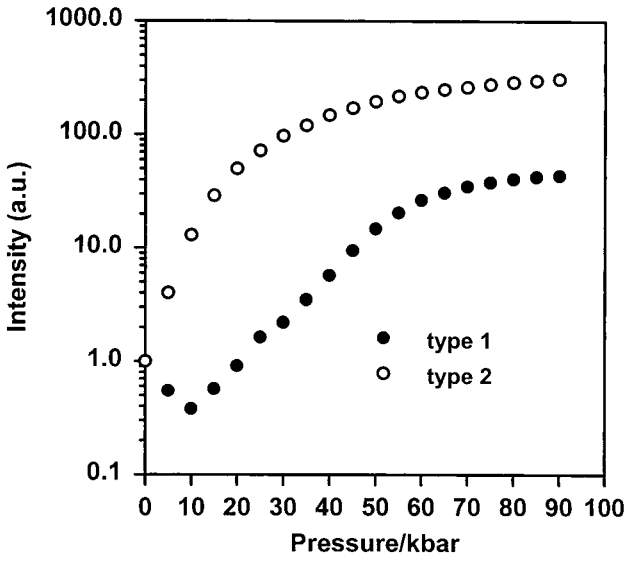

Figure 9. SHG intensity vs pressure (normalized to 1 atm value) for BMC at the angle for maximum intensity at 1 atm—averaged over several loads for two crystal types.

For the powder no angle dependence of the intensity was observed at any pressure. In Figure 10we present the change of intensity with pressure normalized to 1 atm averaged over three loads. The intensity maximizes near 45 kbar at a value 1.8 ± 0.2 times the 1 atm value. This is clear evidence for a phase transition in the region 35−50 kbar. In the crystal the intensity rise with pressure (Figures 8 and 9) is so steep as to obscure this evidence.

For the crystals, when the pressure is released from a pressure less than that of the phase transition (∼35 kbar), the intensity change is reversible. When pressure is released from ∼80 kbar, the sample relaxes to conditions just above the phase transition (∼40 kbar). There is a further reduction of intensity by a factor of 1.5−2 over 2−3 days, but it does not approach the original 1 atm intensity.

Figure 11exhibits optical absorption spectra for the powder at a series of pressures. Up to 47 kbar there is a consistent red shift with no significant change in intensity or shape of the edge. At higher pressures there is distinct drop in intensity and a change in shape of the edge, consistent with the phase transition

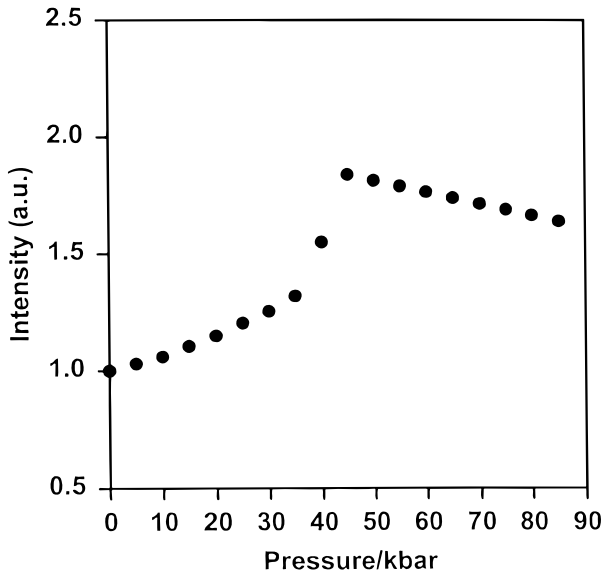

Figure 10. SHG intensity vs pressure (normalized to 1 atm value) for BMC powder averaged over several loads.

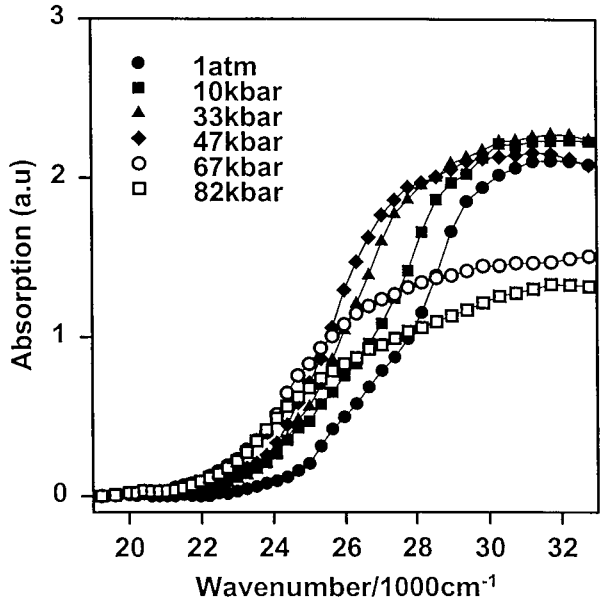

Figure 11. Optical absorption spectra for BMC at a number of pressures.

indicated for the SHG measurements on powder. When the pressure is released, the peak shifts to its original position, but it does not regain intensity.

MNA. In our previous paper[7] we presented some results for SHG on MNA as a powder or as a crystal almost certainly damaged by our method of operation. Initially the intensity was relatively high. There was a slight increase in the first 2−3 kbar and then a drop by a factor of ∼20 in the range 5−40 kbar with little or no pressure effect beyond that. It is now clear from a more detailed analysis of the optical absorption data that there is significant absorption even at 20 kbar and that beyond ∼30 kbar the decrease is dominated by self-absorption of the sample.

Here we present data on carefully loaded single crystals to 30 kbar pressure. The crystals were thin needles, and the orientation was controlled to the degree discussed for ABP above. We discuss first the intensity vs pressure as presented in Figure 12. Immediately upon application of pressure there is a sharp increase in intensity by a factor of ∼20 in 10 kbar.

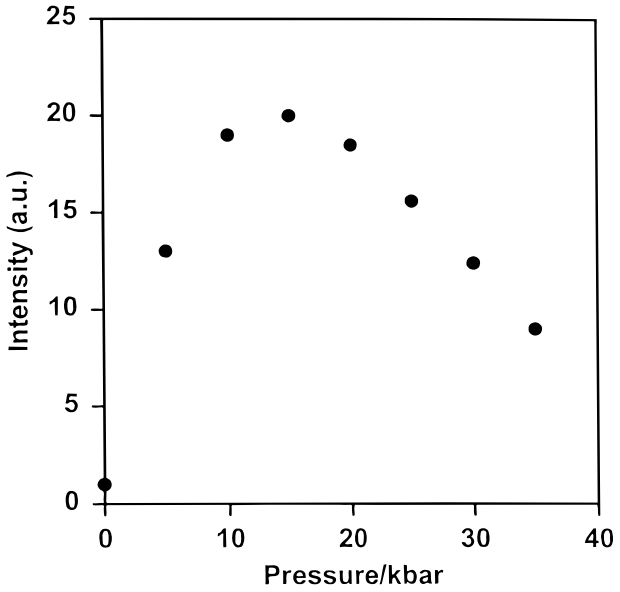

Figure 12. SHG intensity vs pressure normalized to 1 atm for MNA crystal—averaged over several loads and all angles of polarization of the laser beam.

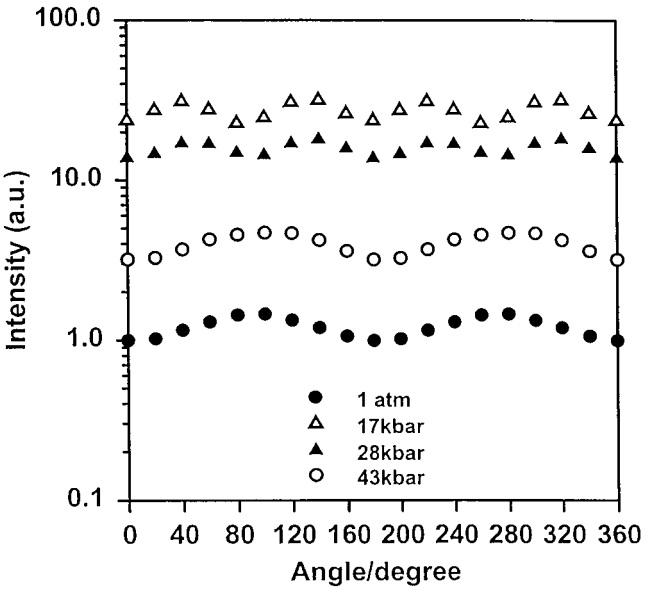

Figure 13. Typical SHG intensity as a function of polarization angle of the laser beam for MNA crystal for several pressures.

Beyond 15 kbar there is a decrease in intensity which continues to 50−60 kbar as for the powder data[7] and is undoubtedly in significant part associated with self-absorption. There appears to be no important effect of orientation in the plane perpendicular to the long axis. There is no doubt that there is a phase transition involved. This can be seen also in the plot (Figure 13) of typical SHG intensity vs angle of polarization. At 1 atm there are two maxima, while at 17 and 28 kbar one can clearly see four maxima. It is of interest to note that by 43 kbar the shape has returned to that at 1 atm. Upon release of pressure the intensity and angle dependence returned to that corresponding to about 8−10 kbar but never returned to the initial value.

Because of the strong effect of absorption, the studies of MNA are more restricted than those for ABP and BMC, and we do not include MNA in our discussion below.

Discussion

There have been a variety of high-pressure X-ray studies of organic materials. However, those involving extraction of lattice parameters of complex crystals have been largely limited to 10−15 kbar. In any case, facilities for measuring the effect of pressure on the lattice parameters of the materials involved in this paper over a suitable pressure range are not available to us. Thus, a quantitative discussion of these optical studies in terms of the theory of SHG efficiency is not, at present, possible.

Bridgman[13,14] showed that a number of solid benzene derivatives compress by 18−21% in 40 kbar. Thus, one can expect that there will be significant volume changes in the crystals studied here. For the monoclinic structure these changes will almost certainly be anisotropic. There should also be significant changes in the refractive indices associated with the fundamental and second harmonic waves propagated in any direction in the crystal, and these changes will be orientation dependent.

SHG conversion efficiency in the plane-wave fixed-field approximation can be expressed as[15]

$$\frac{I^{2\omega}}{I^{\omega}} \approx \frac{d_{\text{eff}}{}^2 L^2 I^{\omega}}{(n^{\omega})^2 n^{2\omega}} \left[\frac{\sin^2(\Delta kL/2)}{(\Delta kL/2)^2} \right] \tag{1}$$

where $I^{2\omega}$ and I^{ω} are the second harmonic and laser intensities, respectively, d_{eff} is the effective nonlinear coefficient, L is the thickness of the nonlinear crystal in the direction of the incident beam, $n^{2\omega}$ and n^{ω} are the refractive indices respectively for the second harmonic and fundamental waves, and Δk is the wave vector mismatch between the coupled fields:

$$\Delta k = \frac{2\pi}{L_c} = \frac{4\pi}{\lambda}(n^{2\omega} - n^{\omega}) \tag{2}$$

L_c is the coherence length (a measure of the maximum crystal length that is useful for SHG in the presence of phase mismatch, i.e., when $\Delta k \neq 0$).

A number of terms in eq 1 must be pressure sensitive. However, the changes in L, n^{ω}, and $n^{2\omega}$ (assuming that something like the Lorenz−Lorentz relationship can be applied to anisotropically compressible crystals), while quite measurable, will not yield changes of SHG efficiency of the magnitude observed. (The above comment does not, of course, apply to the difference $(n^{2\omega} - n^{\omega})$.) In any case, since L will decrease and the refractive indices in the denominator will increase, the effect of pressure will be to decrease the factor L^2/n^3.

There is no really satisfactory way of establishing quantitatively the effect of pressure on d_{eff} for these crystals. However, for BMC powder the SHG efficiency is independent of the angle of polarization of the laser beam at all pressures; therefore, there is no apparent effect of Δk. Equation 1 was developed for crystals and in transmission. The equations for powders involve variables[6] not available to us. As a very crude approximation, however, it is useful to apply eq 1 to our data for BMC powder in the region below the phase transition to estimate roughly the change in d_{eff} with pressure. We used the $p-v$ data of Bridgman[14] for 4-nitroaniline—a material having the charge-transfer characteristics of SHG materials. The average 1 atm refractive index can be corrected for pressure using the Lorenz−Lorentz formula. Thus, L^2/n^3 can be calculated as a function of pressure, normalized to 1 atm. From these values and the normalized intensity changes one obtains the results exhibited in Table 1for BMC. The refractive indices for BMC were taken from[12] and averaged over the three directions. $n_0{}^3$ was calculated as indicated in the table. The same treatment would apply to ABP up to 20 kbar if refractive index data were available.

TABLE 1: Calculation of Change of d_{eff} with Pressure for BMC Powder[a]

P (kbar)	I/I_0	$(L^2/n^3)/(L^2/n^3)_0$	$d_{eff}/(d_{eff})_0$
0	1.00	1.00	1.00
10	1.06	0.843	1.12
20	1.14	0.760	1.23
35	1.30	0.669	1.39

[a] Note: $n_0^3 = [(n_0^{\omega})^2 n_0^{2\omega}]$. The subscript 0 refers to atmospheric pressure.

The most promising term for explaining our results is that in the square brackets. As shown first by Maker et al.[16] and elaborated in many monographs and textbooks (e.g., refs 17 and 18), the function has a very sharp, strong maximum at $\Delta k = 0$. In terms of the angle between the fundamental beam and the phase matching direction, the function goes from nearly zero to one in ~0.06°. There are much smaller subsidiary maxima at larger values of Δk.

For constant Δk the product ΔkL will decrease by 5−10% in 90 kbar depending on anisotropy in the compressibility. However, the major change in the product is probably due to changes in Δk caused by the anisotropic compression. A phase transition that results in a different point group would enhance or oppose this effect. In essence, we have introduced the "pressure tuning" of the anisotropic refractive indices and therefore of Δk.

A plausible scenario can be developed for BMC that indicates that the crystal at 1 atm has a value of ΔkL such that the effects of anisotropic compression could result in very large changes in SHG efficiency. As mentioned earlier, the BMC crystals in the cell have their crystallographic z axis parallel to the laser beam. Let us assume as a first approximation that the (optical) z axis lies along the perpendicular to the crystal plate surface. The largest active component of the **d** matrix would then be d_{26} (d_{212}). Then the major contribution to the SHG intensity is of the form

$$I^{2\omega} \approx {d_{26}}^2 \,\mathrm{Sinc}^2\left[\frac{2\pi L}{\lambda}\left({n_y}^{2\omega} - \frac{{n_x}^{\omega} + {n_y}^{\omega}}{2}\right)\right] \quad \text{where Sinc} = \frac{\sin\theta}{\theta} \quad (3)$$

Using the 1 atm refractive indices[15] and an initial thickness of 20 ± 5 μm,

$$I^{2\omega} = {d_{26}}^2 \,\mathrm{Sinc}^2(3.5 \pm 0.5) \quad (4)$$

As can be seen from Figure 14, the decrease in L plus a modest decrease in Δk would indeed result in a large increase in SHG intensity with increasing pressure. The crystals were thin (20 ± 5 μm), and it was difficult to measure the thickness accurately without damaging them. If the type 1 crystals averaged a little thicker than the type 2, the decrease in ΔkL at low pressure could account for the initial decrease in SHG intensity as well.

Conclusions

Pressure can have a dramatic effect on the SHG efficiency of organic crystals. In the case of ABP and BMC increases of 2−3 orders of magnitude over a pressure range less than 100 kbar are observed. The results can be explained qualitatively in terms of a theoretical model for SHG efficiency. The term $[\sin^2(\Delta kL/2)]/(\Delta kL/2)^2$, in which L is the thickness of the crystal in the light path and Δk is the mismatch in the wave vector between the coupled fields, varies very rapidly with Δk near $\Delta k = 0$. In terms of the angular difference $\Delta\theta$ between the fundamental beam and the phase matching direction, a change of 0.06° can change the efficiency by 3−4 orders of magnitude. Given the undoubtedly anisotropic compressibility of monoclinic crystals, such a change in phase matching direction is easily conceivable.

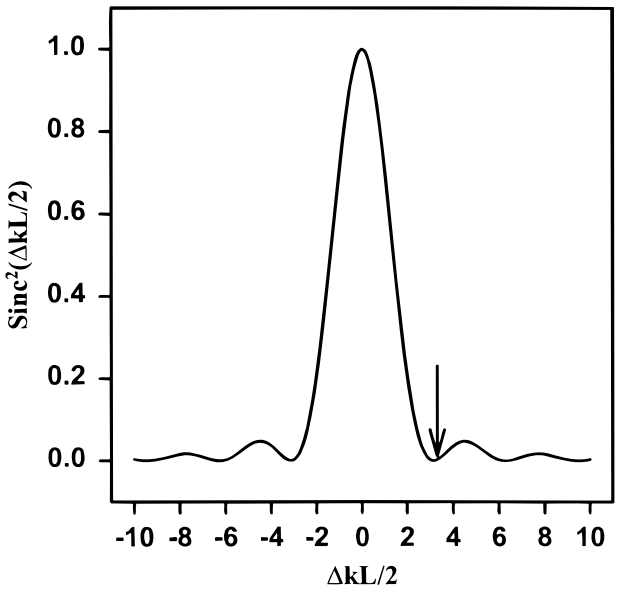

Figure 14. Sinc($\Delta kL/2$) vs $\Delta kL/2$. The arrow indicates the approximate 1 atm value for $\Delta kL/2$ for BMC.

Acknowledgment. The authors are pleased to acknowledge continuing support from the U.S. Department of Energy, Division of Materials Science Grant DEF602-96ER45439, through the University of Illinois at Urbana-Champaign Frederick Seitz Materials Research Laboratory. Most of the research was performed in the MRL Laser Laboratory.

References and Notes

(1) *Materials for Nonlinear Optics (Chemical Prospectives);* Marder, S. R., Sohn, J. E., Stucky, G. D., Eds.; ACS Symposium Series 455; ACS Press: Washington, DC, 1983.
(2) *Principles and Applications of Nonlinear Optical Materials;* Munn, R. W., Ironside, C. N., Eds.; Blackie Academic and Professional: London, 1993.
(3) *Non-linear Optical Materials;* Kuhn, H., Robillard, J. O., Eds.; CRC Press: Boca Raton, FL, 1992.
(4) *Organic Materials for Norlinear Optics (II);* Hahn, R. A., Bloor, D., Eds.; The Royal Society of Chemistry: London, 1991.
(5) *Organic Materials for Norlinear Optics (III);* Hahn, R. A., Bloor, D., Eds.; The Royal Society of Chemistry: London, 1993.
(6) Kurtz, S. K.; Perry, T. T. *J. Appl. Phys.* **1968**, *39*, 3798.
(7) Yang, G.; Li, Y.; Dreger, Z. A.; White, J. O.; Drickamer, H. G. *Chem. Phys. Lett.* **1997**, *280*, 375.
(8) Kohler, E. P.; Chadwell, H. M. In *Organic Syntheses*; Gilman, H., Ed.; John Wiley & Sons: New York, 1941; Collective Vol. 1, p 78.
(9) Piermarini, G. J.; Block, S. *Rev. Sci. Instrum.* **1975**, *46*, 973.
(10) Bray, K. L.; Drickamer, H. G.; Schmitt, E. A.; Hendrickson, D. N. *J. Am. Chem. Soc.* **1989**, *111*, 2849.
(11) Lang, J. M.; Drickamer, H. G. *J. Phys. Chem.* **1993**, *97*, 5058.
(12) Zhang, G.; Kinoshita, T.; Sasaki, K.; Goto, Y.; Nakayama, M. *J. Cryst. Growth* **1990**, *100*, 411.
(13) Bridgman, P. W. *Proc. Am. Acad. Arts Sci.* **1945**, *76*, 9.
(14) Bridgman, P. W. *Proc. Am. Acad. Arts Sci.* **1948**, *76*, 71.
(15) *Handbook of Nonlinear Optical Crystals;* Dimitriev, V. G., Guradyan, G. G., Nikogosyan, D. N., Ed.; Springer-Verlag: Berlin, 1997.
(16) Maker, P. D.; Terhune, R. W.; Nissenoff, M.; Savage, C. M. *Phys. Rev. Lett.* **1962**, *8*, 21.
(17) Munn, R. W. In *Nonlinear Optical Materials;* Kuhn, H., Robillard, J. O., Eds.; CRC Press: Boca Raton, FL, 1992; p 10.
(18) Yariv, A. In *Quantum Electronics*, 2nd ed.; J. Wiley & Sons: New York, 1975; p 427.